

ASYNCHRONY OF MOSSY FIBRE INPUTS AND EXCITATORY POSTSYNAPTIC CURRENTS IN RAT HIPPOCAMPUS

BY RONALD B. LANGDON, JON W. JOHNSON
AND GERMAN BARRIONUEVO*

*From the Departments of Behavioral Neuroscience and Psychiatry, University of
Pittsburgh, Pittsburgh, PA 15260, USA*

(Received 29 October 1992)

SUMMARY

1. Excitatory postsynaptic currents (EPSCs) were studied by whole-cell voltage-clamp recording (WCR) from pyramidal cells in the CA3 field of rat hippocampal slices. Input from mossy fibres was evoked by stimuli applied to stratum granulosum ('dentate gyrus stimulation'). This often resulted in complex, multi-component EPSCs with rise times as long as 5.0 ms (mean = 2.5 ms). In contrast, individual EPSC components typically had rise times between 0.3 and 1.0 ms.

2. To isolate monosynaptic, mossy fibre-driven EPSC components, slices were exposed to 'suppressing' media that reduced response amplitudes by 64–88%. In five out of six cases, long EPSC rising phases (> 3 ms) retained the same shape during suppression. This implied that EPSCs were driven by asynchronously active mossy fibre inputs.

3. From latencies of antidromically driven granule cell population spikes (GCPSs) a mean conduction velocity of 0.67 m/s was inferred. Conduction distance had practically no correlation with GCPS duration, implying that velocity dispersion was small and did not desynchronize mossy fibre impulses. EPSC components exhibited 'surplus' latency; they occurred 0.9–4.8 ms after latencies expected on the basis of direct conduction distances.

4. Mossy fibre volleys (MFVs) were evoked by dentate gyrus stimulation and studied with neurotransmission disabled. MFV negative phases lasted from 2.5 to 4.5 ms and had multiple components. By comparison, negative phases of Schaffer collateral fibre volleys (SCFVs) were always simple in shape and lasted 1.5 ms or less. MFV components had surplus latencies similar to those of EPSC components. Late MFV components did not require high stimulus intensities.

5. Widespread activation of granule cells occurred when stimuli were applied to single loci in the stratum granulosum. This implies that such stimuli elicit antidromic impulses in hilar collaterals of mossy fibres, which could result in activation of orthodromic impulses in mossy fibre trunks that had not been stimulated directly. After anti-, then orthodromic conduction, impulses would arrive in the CA3 subfield with 'surplus' latency.

* To whom reprint requests should be sent at the Department of Behavioral Neuroscience, 446 Crawford Hall, Pittsburgh, PA 15260, USA.

6. When cuts were made in the hilus to prevent anti-/orthodromic conduction, MFV durations were reduced, but only to a small extent. This implies that surplus latency and asynchrony arise in part by anti-/orthodromic conduction, and partly by a mechanism that is intrinsic to mossy fibres or their 'giant' boutons.

7. Because of desynchronization of mossy fibre inputs, there probably are significant differences between kinetic properties of averaged, compound mossy fibre EPSCs and those of unitary mossy fibre EPSCs (i.e. currents driven by input from single presynaptic axons). It is likely that some rapidly rising components within compound EPSC waveforms are unitary EPSCs.

INTRODUCTION

The 'mossy fibre synapse' in the hippocampus mediates neurotransmission between granule cells of the dentate gyrus and pyramidal cells in the CA3 subfield of hippocampus. Because it is close to the cell soma, this synapse has been proposed as ideal for application of voltage-clamp methodology to the study of cortical glutamatergic neurotransmission (Brown & Johnston, 1983; Johnston & Brown, 1983; Brown & Zador, 1990). In addition, there is considerable interest in this synapse as a model for the study of synaptic plasticity, in that it exhibits an NMDA receptor-independent form of long-term potentiation (reviewed by Johnston, Williams, Jaffe & Gray, 1992). Physiological studies of this synapse generally depend upon bulk stimulation of mossy fibres and require accurate discrimination between pure 'mossy fibre EPSCs' (excitatory postsynaptic currents driven entirely by mossy fibre input) and responses that are contaminated by polysynaptically mediated input. Such discriminations are made based upon expectations regarding the characteristic kinetics of pure mossy fibre EPSCs. Specifically, these are expected to rise and decay monophasically and to have a rising phase lasting no longer than 3 ms (Brown & Johnston, 1983; Claiborne, Xiang & Brown, 1993). In most previous studies, responses not conforming to these criteria have been rejected. However, it has remained unclear to what extent samples of EPSCs with rise times less than 3 ms include contaminated responses, and to what extent there occur uncontaminated mossy fibre EPSCs with rise times greater than 3 ms. Because of uncertainty regarding the extent of polysynaptic contamination, the true distribution of mossy fibre EPSC rise times remains unknown.

Even if the 3 ms upper boundary were to be accepted as definitive, a compelling problem would remain, as was discussed by Williams & Johnston, who performed the most definitive study to date of mossy fibre EPSC kinetics (1991). Within their sample of responses that met the 3 ms criterion, 41% of rise times fell between 2.0 and 3.1 ms. There is no ready explanation why mossy fibre EPSC rise times should be this long. Long rise times in their sample did not appear to be a consequence of distal synaptic input because rise times and decay times were essentially uncorrelated. Much shorter rise times occur at other synapses that could not be much closer to cell somata than are mossy fibre synapses (Finkel & Redman, 1983; Nelson, Pun & Westbrook, 1986). Moreover, most collateral inputs (i.e. inputs from axon collaterals of other pyramidal cells) are thought to be electrotonically farther from the soma than are mossy fibre inputs, and yet collateral-driven EPSCs often rise as quickly as mossy fibre EPSCs (Hestrin, Nicoll, Perkel & Sah, 1990; Langdon,

Johnson & Barrionuevo, 1991; Williams & Johnston, 1991). Finally, the rise time has been observed to vary between only 0.3 and 1.5 ms for mossy fibre EPSCs thought to be unitary (Jonas & Sakmann, 1991).

Existing data could be explained by a hypothesis that bulk electrical stimulation applied to the dentate gyrus results in asynchronous activity of mossy fibre inputs to hippocampal pyramidal cells. In this study, we have examined this hypothesis using a combination of approaches including whole-cell recording (WCR) of low-amplitude EPSCs and analysis of impulse conduction in mossy fibres. Our data lead to the conclusion that mossy fibre impulses initiated by bulk stimulation in dentate gyrus are conducted along two different routes to the hippocampus, with the result that conduction distances differ widely and mossy fibre inputs are active asynchronously. However, additional latency and asynchrony appears to be the result of some inherent property of mossy fibre axons or terminal boutons. We conclude that asynchronous presynaptic activity is a major determinant of the duration of the rising phase of mossy fibre EPSCs under normal conditions of study.

We have presented some of these data previously in preliminary form (Langdon *et al.* 1991; Langdon, Johnson & Barrionuevo, 1992).

METHODS

Solutions, chemicals and slices

Slices were prepared and maintained in artificial cerebrospinal fluid (ACSF) composed of (mM): NaCl, 114; KCl, 3; CaCl₂, 3; MgCl₂, 3; Na₂SO₄, 1.2; D-glucose, 10; Hepes, 10; Phenol Red, 0.01; NaHCO₂, 25; sodium phosphate buffer (pH 7.0), 1; and sufficient (~2.5 mM) NaOH to bring pH to 7.3–7.4 when bubbled with carbogen (95% O₂, 5% CO₂). We did not add GABA antagonists to our ACSF because block of inhibitory postsynaptic currents (IPSCs) was not necessary under the conditions of this study (see Results, Fig. 2), and including GABA antagonists would be likely to increase the incidence of polysynaptic contamination of mossy fibre-evoked currents. We refer to ACSF with all Ca²⁺ replaced by Mg²⁺ as 'Ca²⁺-free' (final [Mg²⁺] = 6.0 mM). Because EPSCs were recorded primarily to determine when input occurred, WCR pipettes were filled with a solution chosen to maximize recording stability and cell yield, rather than one more supportive of postsynaptic metabolism. Specifically, this solution contained (mM): CsF, 120; CsCl, 10; EGTA, 10; Hepes, 10; adjusted with CsOH to pH 7.35 ± 0.5. In addition to anaesthetics (see below), two pharmacological agents were used: 2-amino-5-phosphonovalerate (APV) from Cambridge Research Biochemicals (Gadbrook Park, UK) and 6-cyano-7-nitroquinoxaline-2,3-dione (CNQX) from Tocris Neuramin (Bristol, UK).

Transverse hippocampal slices, 400 μm thick, were prepared from male Sprague–Dawley rats (Zivic–Miller, PA, USA; 100–200 g) following procedures similar to those used previously in the preparation of neocortical slices (Langdon & Sur, 1990, 1992). Animals were deeply anaesthetized by intramuscular injection of ketamine HCl (100 mg/kg) and acepromazine maleate (10 mg/kg) prior to being killed by decapitation. All slices were derived from the same region of hippocampus, about 2–3 mm from the septal termination of the septotemporal axis (the same region and orientation as indicated in Fig. 2 of Amaral & Witter, 1989). Physiological recordings were performed with slices immobilized on a submerged nylon net in ACSF at 33 °C.

Cytoarchitectural boundaries and stimulation

Our use of anatomical terms and divisions is after Lorente de Nó (1934). Outlines of hippocampal slices and electrode positions were traced at 145 × final magnification from a video monitor, using a 4 × objective on an upright compound microscope (Model Laborlux 12, Leitz, Wetzlar, Germany) coupled to a video camera. S. granulosum, s. pyramidale, white matter tracts and stimulus electrodes were clearly visible in living slices.

Except when stated otherwise, stimuli were applied to the supragranular blade of the s. granulosum with the stimulus electrode oriented so that its shaft did not pass through the hilus.

Perforant path axons were lesioned in many experiments (illustrated as 'cut 2' in Fig. 7A), since it was plausible that some of these would be activated by stimuli applied to the s. granulosum. To avoid polysynaptic contamination of EPSCs, we selected levels of stimulation that evoked responses of minimal amplitude. In previous studies in which mossy fibre EPSCs were examined by single-electrode voltage-clamp (SEVC), responses were generally about 1 nA in amplitude (Brown & Johnston, 1983; Barrionuevo, Kelso, Johnston & Brown, 1986). By using WCR, however, we could study EPSCs 2- to 20-fold lower in amplitude and yet have single-trial (rather than averaged) response waveforms that were large compared with the background noise (Figs 1 and 2). Stimulus currents ranged from 0.2 to 5.0 mA (by 50 or 100 μ s), with a mean of 0.98 mA. In order to reach slices under the water immersion microscope objective, stimulus electrodes were situated side by side for 5–10 mm, about 200 μ m apart and submerged in ACSF. Due to these conditions, there was probably a large stray capacitance, and consequently applied stimulus currents were probably much larger than currents actually delivered to the slices.

Whole-cell recording (WCR) and extracellular recording

Cell 'cleaning' and WCR were performed under visual observation using a 40 \times water immersion objective (Carl Zeiss, Germany) following procedures previously described by Edwards, Konnerth, Sakmann & Takahashi (1989), with two modifications. (1) To accommodate the use of thick slices (400 μ m in this study), cell images were monitored with a contrast-enhancing video system (Model CCD-72S, Dage-MTI, Michigan City, IN, USA). (2) WCR was performed preferentially on those cells for which only the soma had been exposed by cleaning because mossy fibre synapses are located on proximal dendrites. WCR pipettes were neither coated nor fire-polished. Pipette resistances prior to seal formation were 3–6 M Ω . All WCR was performed in the voltage-clamp mode with cells maintained at a nominal holding potential of -70 mV, except when stated otherwise. 'Resting' potentials were within 10 mV of zero ($n = 5$), as expected because the WCR pipettes contained Cs⁺. The mean holding current was -0.60 ± 0.36 nA, implying a mean input impedance of 120 M Ω . Series resistance compensation was not used. If it is assumed that a typical pipette series resistance was 9 M Ω (twice the typical resistance prior to seal formation), then actual membrane potentials would have been 5 ± 3 mV more positive than the command holding potential of -70 mV. During the peak of a typical EPSC in this study, there would have occurred an additional voltage error of 2 mV. Such discrepancies between actual and command potentials would have no significant effects upon EPSC rising phase duration and complexity, and therefore would have no bearing upon the conclusions drawn in this study. Long EPSC rise times were clearly not a consequence of poor clamp bandwidth (which would occur in cases of very high and uncompensated series resistance) because rising phases included rapidly rising components (see Results). EPSC rise times were measured as the interval on the rising phase between 10 and 90% of peak amplitude.

Extracellular potentials were recorded using low-resistance glass micropipettes (2–7 M Ω) filled with ACSF. All extracellular potentials were recorded at least 100 μ m from cut edges of slices to minimize 'edge effects' (Klee & Rall, 1977; see also Langdon & Sur, 1990). Because glass electrode tips were not visible during recordings, tip positions were determined as follows. After recording from a site, the electrode was withdrawn a measured distance along the axis of entry until it cleared the slice, then withdrawn from the slice along the line of sight, and finally advanced by the previously measured distance so that the tip would be situated directly over what had been the recording position. Its position was then traced from the video monitor.

Data acquisition and statistical conventions

WCR was performed with an Axopatch 1C patch-clamp amplifier (Axon Instruments, Burlingame, CA, USA) with the low-pass filter corner frequency (-3 dB) set at 5 kHz. Waveforms were analysed both on-line and after storing on videocassette tape (using a Neuro-corder Model DR-484, Neuro Data Instrument Corp., New York, USA). For computer-based analysis, data were digitized at 6.67 or 10 kHz. Extracellular potentials were recorded using the Axopatch 1C, the Model 5A from Getting Instruments (Iowa City, IO, USA), or the BMA-831 from CEW, Inc. (Ardmore, PA, USA). These data were low-pass filtered at either 5 or 10 kHz and digitized at 13.33 kHz.

Sample population parameters are given as means ± 1 standard deviation, except when stated otherwise.

RESULTS

Complex EPSC rising phases

EPSCs were recorded from twenty-seven pyramidal cells in the CA3b subfield in twenty-five slices from twenty-four animals. Within this sample, amplitudes of averaged responses from individual cells ranged from 11 to 502 pA; the mean amplitude was 223 pA. During a typical recording, there were complexities in individual (single-trial) evoked responses that were partly or wholly obscured by response averaging. More specifically, single-trial rising phases were often inflected in a way that implied summation of multiple, asynchronous EPSC components (Fig. 1). Figure 1*Ba* shows a recording in which these component were unusually distinct and variable from one trial to the next, while Fig. 1*C* shows an example of EPSCs more typical of those in our sample. These individual EPSC components had rising phases lasting 0.3–1.0 ms, and the largest appeared to add as much as 350 pA to the amplitude of the total response. These components were a specific characteristic of responses to stimulation of the dentate gyrus; responses to fimbria stimulation recorded in the same cell generally were more simple in shape (Fig. 1*Bb*) ($n = 15$). Despite the obscuring effect of response averaging, rising phase inflexions were also apparent in some averaged response waveforms (e.g. Figs 1*Cb* and 3*B*).

Overall rise times of averaged EPSCs in our sample were similar to those in previous studies ('overall' referring to entire response waveforms, irrespective of inflexions). In the present study, rise times ranged from 0.6 to 5.0 ms, with a mean of 2.5 ± 1.2 ms. The rise time was 3 ms or less for 60% of our averaged response waveforms, 2 ms or less for 35%, and 1 ms or less for 13%. Thus, roughly half of the EPSCs in the present study would have satisfied the 3 ms rise time criterion that was used in previous studies. Some of the complex EPSCs in the present study would have been among the rejected half. Figure 1*Ba* provides an example; the overall rise time for EPSCs from this recording was 3.8 ms (based on an average of forty responses, not shown). However, we also observed many EPSCs that satisfied the 3 ms criterion and yet were clearly the sum of multiple components. The responses in Fig. 1*C* are an example. EPSCs during this recording rose in only 1.2 ms, on average. However, many of the unaveraged responses recorded from this cell were clearly inflected, and the rising phase of the averaged response was slightly inflected near its mid-point. Even with the most rapidly rising and falling EPSCs in our sample (Fig. 1*D*; overall rise time = 0.6 ms), there were individual trials in which the rising phase appeared to be composed of responses to slightly asynchronous inputs (arrow). These findings suggest that asynchronous components may have been present, but undetected, in previous studies that used SEVC.

Either of two explanations could account for the asynchrony. Some of these rapid components may have been the result of polysynaptic response contamination, provided that it were possible for collateral-driven components to have the observed rapid kinetics. Alternatively, all rapid components may have been driven by input from mossy fibres alone, provided that these inputs were active asynchronously. Subsequent experiments sought to resolve which components were driven by mossy fibre inputs, and which by collateral inputs.

We considered that latencies could be useful in making this distinction. Based on

an average conduction velocity of 0.67 m/s (see below) and on apparent conduction distances (that is, distances between stimulation and recording sites), conduction delay latencies were estimated and were compared with observed latencies of EPSC components (Figs 1 and 3). We refer to differences between observed latency and

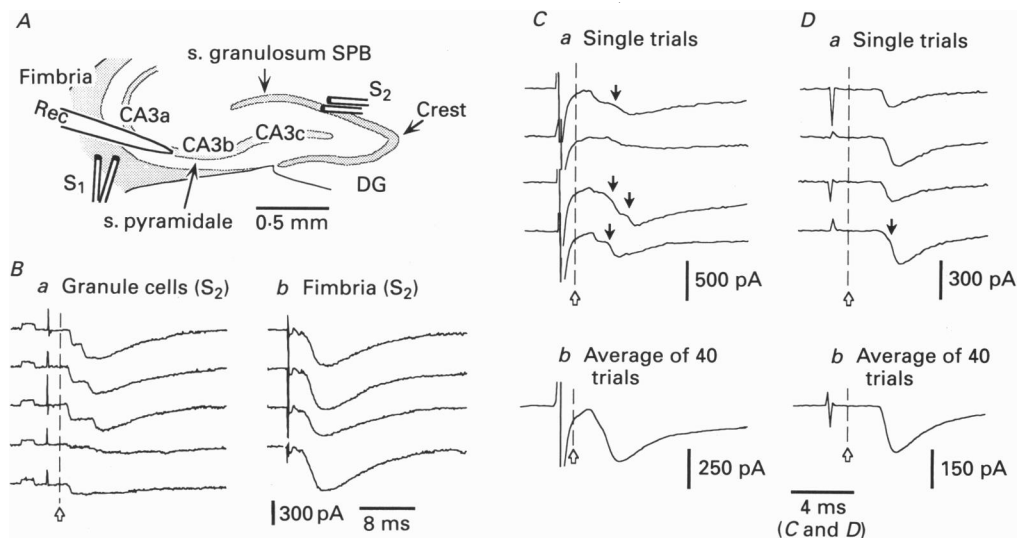


Fig. 1. EPSCs evoked by stimulation of mossy fibres. *A*, anatomy of the slice from which the data in *B* were recorded. Stimulation electrodes are indicated as S_1 and S_2 , and the WCR pipette as 'Rec'. Other abbreviations are: SPB, suprapyramidal blade; DG, dentate gyrus. *B*, EPSCs evoked in consecutive trials in which stimuli were applied alternately via electrodes S_1 and S_2 . The vertical scale and time base in *Bb* pertain to both *Ba* and *Bb*. The rectangular calibration waveform ($50 \text{ pA} \times 2.0 \text{ ms}$) that begins each trace in *Ba* was added to the amplifier output; it was not applied to the cell. *C*, EPSCs from a different slice and cell. Stimuli were applied to the s. granulosum near the crest of the dentate gyrus. *D*, atypically brief EPSCs from a third slice and cell (stimulus position similar to that shown in part *A*). In *Ca* and *Da*, filled downward arrows indicate rising phase inflexions. For the averaged waveforms in *Cb* and *Db*, the vertical gain is doubled. In this and subsequent figures, latency directly attributable to conduction delay is indicated by vertical dashed lines above unfilled arrows. Variability in the stimulus artifact (as in *Da*) occurred because the artifact was brief compared with the digitizing period.

estimated conduction delay as 'surplus' latency. Surplus latencies were between 0.9 and 2.6 ms for initial EPSC components and ranged up to 4.8 ms for the later components. Thus, no EPSC components occurred too early to have been driven by mossy fibre input, as could have occurred if responses were contaminated by polysynaptic inputs conveyed by collateral axons conducting much faster than mossy fibres. On the other hand, many EPSCs and EPSC components had surplus latencies so large that they were difficult to attribute to pure monosynaptic, mossy fibre input, despite rapid waveform kinetics. Figure 1*D* provides an example of such an EPSC. It had a long surplus latency of 2.1 ms, yet its very rapid kinetics and simple shape would otherwise have made it an ideal 'mossy fibre EPSC'. These data implied either that there were rapid non-mossy fibre EPSCs driven by polysynaptic

input, or else that a highly variable and unidentified factor played an important role in determining latency of mossy fibre EPSCs.

Response complexity was generally not the result of polysynaptic contamination

Hypothetically, there are two kinds of polysynaptically activated input that could have contaminated our recordings. One of these would be polysynaptically mediated

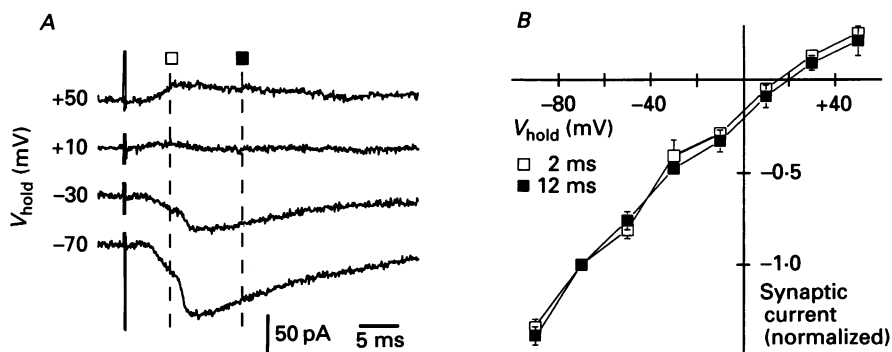


Fig. 2. The shape of postsynaptic current as a function of holding potential. *A*, typical single-trial response waveforms at the four holding potentials indicated at left (V_{hold}). *B*, a current *versus* voltage (I - V) plot of the mean normalized currents in five cells. Current amplitudes were measured at the two latencies indicated in part *A* (vertical dashed lines under open and filled squares), and each was normalized with respect to the evoked current at -70 mV. For all cells combined, the mean synaptic current at -70 mV was -93 pA 2 ms after onset (range: -37 to -174 pA), and -114 pA 12 ms after onset (range: -61 to -216 pA). The vertical error bars represent ± 1 s.e.m. Where the error bars are absent, the s.e.m. was less than the width of the squares.

GABAergic inputs. In previous studies of mossy fibre EPSCs recorded by SEVC, large IPSCs were encountered unless the ACSF included GABA receptor antagonists (Brown & Johnston, 1983; Barrionuevo *et al.* 1986; Griffith, Brown & Johnston, 1986). In the absence of antagonists, postsynaptic current was mostly excitatory for 2–3 ms following onset, but almost entirely inhibitory thereafter, with the IPSC peaking 12 ms after onset (Brown & Johnston, 1983). Under our experimental conditions, GABA_A-mediated IPSCs would have reversed at -63 mV, based on the Goldman–Hodgkin–Katz equation (Bormann, Hamill & Sakmann, 1987; Hille, 1992). To determine whether or not IPSCs were present, we examined responses over ranges of holding potentials that included values between the GABA_A- and glutamate-gated channel reversal potentials (assuming 0 mV for the latter; Ascher & Nowak, 1988). When holding potentials were stepped at 40 ($n = 1$) or 20 mV ($n = 6$) intervals from -90 to $+50$ mV, response waveforms changed in amplitude and polarity, but not appreciably in shape (Fig. 2*A*). Postsynaptic current amplitudes and polarities at 2 and 12 ms displayed nearly identical dependencies upon membrane potential (Fig. 2*B*). We therefore conclude that IPSCs were nearly or wholly absent from our recordings even though our ACSF contained no GABA antagonists. This absence may have been the result of GABA receptor ‘run-down’ (Chen, Stelzer, Kay & Wong, 1990) and destruction of inhibitory inputs to cell somata brought about by ‘cleaning’ cells prior to WCR.

A second possibility would be that our EPSCs with long rise times were evoked by the combined action of mono- and polysynaptic excitatory inputs. To determine whether this was the case, we examined the effects of 'suppressing' media upon the shape of response waveforms for which the rise time exceeded 3 ms. Partial blocking

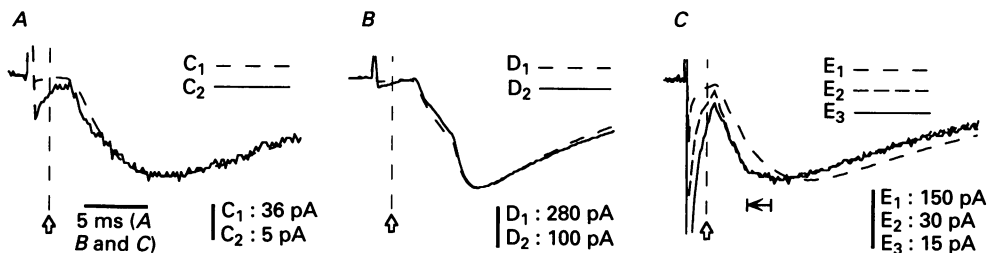


Fig. 3. The effect of suppressing synaptic transmission on EPSC waveforms. Responses recorded before and during suppression are superimposed, with peak amplitude normalization. All waveforms are averages of forty to fifty trials. *A*, EPSC C_1 was recorded in 3 mM Ca^{2+} and Mg^{2+} , and C_2 in 1.5 mM Ca^{2+} , 4.5 mM Mg^{2+} . *B*, EPSC D_1 was recorded in normal ACSF, and D_2 in 1 μ M CNQX. *C*, EPSC E_1 was recorded in normal ACSF, E_3 during the full effect of 3.2 μ M CNQX, and E_2 after partial recovery during wash-out. In this one recording, suppression caused the time of 90% peak amplitude to occur 1.6 ms earlier (horizontal arrow). In *B* and *C* the ACSF included 50 μ M D-APV.

of excitatory transmission throughout a slice would be expected to change the relative contributions made by inputs of differing synaptic order, which would change the shape of the compound EPSC driven by those inputs. Marked reduction in an EPSC's amplitude without a change in shape would imply that it was driven by purely monosynaptic inputs. Synaptic transmission was suppressed with the glutamate receptor antagonists D-APV and CNQX ($n = 3$), or reduction of the ratio of $[Ca^{2+}]$ to $[Mg^{2+}]$ ($n = 3$).

In general, these manipulations had little or no effect on the shape of response waveforms. As examples, the EPSCs in Fig. 3*A* had a mean rise time of 4.1 ms both in normal medium and during suppression to 12% of normal amplitude, and those in Fig. 3*B* retained their rising phase inflexion despite suppression to 36% of normal amplitude. In three of the four other experiments, suppression by 85–90% had no appreciable effect on waveform shape. In one case, the rise time was reduced from 4.0 to 2.4 ms when responses were suppressed by 80 and 90% (Fig. 3*C*). We infer from this atypical result that polysynaptic contamination of mossy fibre EPSCs may have occurred occasionally. However, our more general conclusion was that most long and complex rising phases in this study were not caused by polysynaptic contamination. Subsequent experiments explored possible mechanisms that could be responsible for desynchronizing mossy fibre activity.

Antidromically evoked granule cell population spikes

Hypothetically, mossy fibre activity could become asynchronous due to differences in the velocity of impulse conduction among mossy fibres. We therefore examined temporal characteristics of granule cell population spikes (GCPs) driven by antidromic conduction from stimulus sites in the hippocampus (Fig. 4). In addition,

GCPSs were studied because their amplitudes were expected to provide an index of the extent to which there were intact, interconnecting mossy fibres present between sites in the dentate gyrus and the hippocampus. GCPSs were recorded from fifty-four pairs of stimulation and recording sites in twenty-one slices, with apparent conduction distances ranging from 0.3 to 1.9 mm. GCPS amplitudes of 2 mV or greater were not uncommon, provided that stimuli were applied to CA3b and the conduction distance was less than 1.5 mm (Fig. 4A).

Aside from amplitude differences, all GCPSs were very similar. In 'laminar profiles', GCPSs exhibited the pattern expected for a somatic population spike generated by neurons with asymmetrically oriented dendrites (Lorente de Nó, 1947; Humphrey, 1968; Llinás, Bloedel & Hillman, 1969). There was a large negative potential in the cell body layer and a smaller, biphasic potential in the s. moleculare with its initial phase positive (Fig. 4B). In contrast, the potentials were purely negative in the hilus, and quickly fell in amplitude with increasing distance from the granule cell layer. This pattern implied field potential generation by the granule cell somata, rather than by cells in the hilus or axons passing through the hilus. GCPSs never exhibited appreciable 'jitter' and were similar in shape, amplitude and latency whether recorded in normal ACSF or in an ACSF that disabled synaptic transmission, either by absence of Ca^{2+} (Fig. 4C) or by the presence of D-APV and CNQX (not shown). Taken together, the data strongly indicated that these field potentials were authentic, antidromically driven GCPSs.

Apparent conduction distance was an excellent predictor of GCPS latency. Pooling data from nineteen slices, all latencies fell within ± 0.7 ms of the regression line for latency-to-peak *versus* conduction distance (Fig. 4C); the coefficient of correlation was 0.87. A mean conduction velocity of 0.67 m/s was estimated from the inverse slope of this regression line. The regression line had a *y*-axis intercept of 1.3 ms, a value that probably represents the mean somatic invasion delay.

GCPS waveforms never exhibited multiple maxima and broadened only slightly as a function of conduction distance; the slope of the regression line for the plot of spike half-widths *versus* conduction distances was only 0.21 ms/mm, 7-fold lower than the slope of the regression line for latencies (Fig. 4C). This lack of spike broadening strongly implies that there was little variation in conduction velocity within populations of mossy fibres. Thus it appears that conduction velocity dispersion makes little or no appreciable contribution to the duration and complexity of EPSC rising phases.

Mossy fibre volleys (MFVs)

To assess the time course of activation of mossy fibres in hippocampus more directly, we recorded mossy fibre compound action potentials (mossy fibre 'volleys', MFVs) evoked in a manner identical to that used to evoke EPSCs during WCR. To avoid contamination of MFVs, neurotransmission was blocked either by use of Ca^{2+} -free ACSF or by use of normal ACSF containing glutamate antagonists.

MFV amplitudes ranged from 0.22 to 1.2 mV, with a mean of 0.34 mV ($n = 29$). Because amplitudes were low, our analysis of MFVs relies upon averages of twenty-five to fifty consecutive responses. As a control, Schaffer collateral fibre volleys (SCFVs) were recorded from the same slices as the MFVs, using the same ACSF and

the same (but repositioned) electrodes. SCFV amplitudes ranged from 0.41 to 0.75 mV, with a mean of 0.58 mV ($n = 8$). Both MFVs and SCFVs were dominated by rapid negative potentials that were preceded and/or followed to a variable extent by smaller positive potentials (Fig. 5A). For SCFVs, the negative phase was always

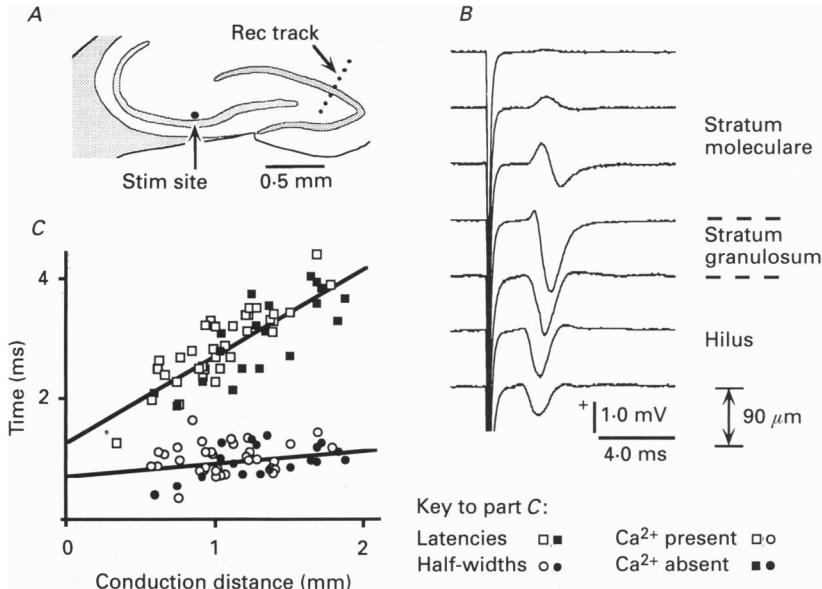


Fig. 4. Granule cell population spikes (GPCSs) in the dentate gyrus evoked by stimuli applied to the s. lucidum. *A*, stimulus ('Stim site') and recording ('Rec track') sites for part *B*. *B*, a laminar profile recorded in normal ACSF at 90 μm intervals along an axis orthogonal to the s. granulosum, as indicated in part *A*. *C*, GPCS latencies (squares) and durations (circles) as a function of the distance between stimulus and recording sites. Data were pooled from nineteen slice preparations, some maintained in normal ACSF (open symbols), others in Ca²⁺-free, high-Mg²⁺ ACSF (filled symbols).

monomodal and brief (Figs 5A and 7B). However, MFV negative phases were always long and complex. They had multiple inflexions and often had multiple negative peaks (Figs 5, 6 and 7). Half-widths did not provide a reliable index of total duration because many MFV negative phases began or ended with low-amplitude components. Fibre volley durations were therefore determined as the interval during which the potential exceeded 10% of peak amplitude. Measured in this manner, the SCFV negative phase duration had a mean of 1.3 ± 0.1 ms and never exceeded 1.5 ms (Fig. 5D). In contrast, the MFV negative phase duration had a mean of 3.2 ± 0.5 ms and ranged from 2.2 to 4.1 ms. Mossy fibre impulse conduction delays were estimated for MFVs in the same way as described above for EPSCs, and are indicated for each MFV illustrated. Typical MFVs began about 1 ms after the estimated conduction delay latency and had additional negative components occurring during the following 2–4 ms. Thus, EPSC rising phase components and MFV negative phase components exhibited similar ranges of 'surplus' latency. In either case, there were components that occurred much later than expected, based on apparent conduction distances.

We considered the possibility that some late 'MFV' components were actually generated by non-mossy fibre axons or cells that had been activated by excessive spread of stimulus current. To ascertain whether all MFV components had spatial distributions consistent with generation by mossy fibres, laminar profiles were

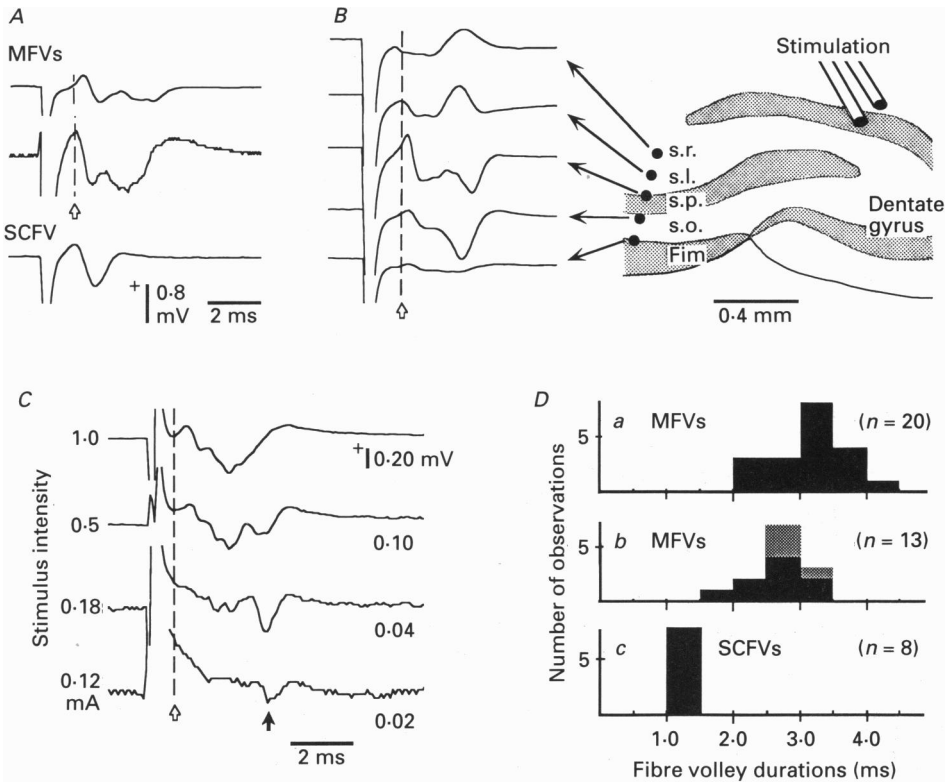


Fig. 5. Mossy fibre volleys (MFVs). *A*, comparison of MFVs with a Schaffer collateral fibre volley (SCFV). For the first MFV, the stimulation site was in the supragranular blade; for the second, it was at the crest of the s. granulosum. The second MFV was recorded in 50 μ M D-APV and 10 μ M CNQX. All other waveforms were recorded in Ca²⁺-free, high-Mg²⁺ ACSF. *B*, a laminar profile recorded along the track indicated. The scale indications in part *A* also apply to part *B*. *C*, MFVs evoked by stimuli of the indicated intensities. The vertical gain for each trace is indicated at the right. The filled arrow indicates an MFV component of long latency that remained present near threshold. *D*, histograms of MFV and SCFV durations: *a*, MFV durations in non-lesioned slices, stimuli applied to the supra- or infrapyramidal blades; *b*, pooled MFV durations in non-lesioned slices, stimuli applied at the crest of the dentate gyrus (grey area; $n = 4$), and in slices with lesions, stimuli applied to the suprapyraximal blade (filled black area; $n = 9$). *c*, SCFV durations.

recorded ($n = 6$). In these profiles, negative potentials occurred only along the trajectory of the mossy fibres (Fig. 5*B*), which course along both the apical and basal sides of s. pyramidale in portions of CA3b and CA3c (Ramón y Cajal, 1911; Lorente de Nó, 1934; Claiborne, Amaral & Cowan, 1986). In other experiments, various levels of stimulus current were applied to determine whether late components were selectively lost near threshold ($n = 12$). We found that late components often

remained present at stimulus intensities that elicited only minimal responses (Fig. 5C). Based on these findings, we conclude that both late and early MFV components were authentic.

The 'anti-/orthodromic' conduction hypothesis: stimulation of mossy fibres via their hilar collaterals

We have presented data that imply retention of synchrony when mossy fibres conduct impulses antidromically, but loss of synchrony when impulses are conducted

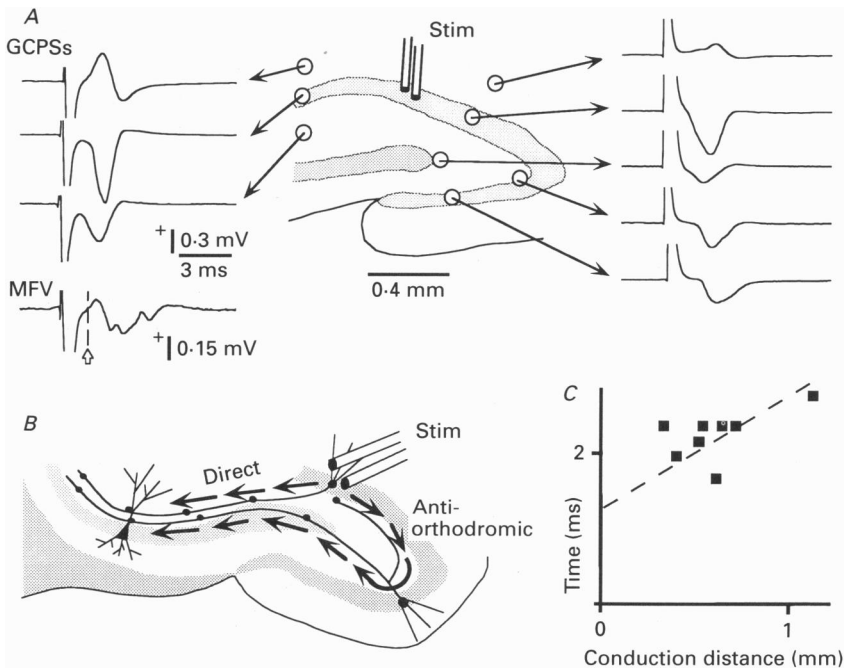


Fig. 6. *A*, granule cell population spikes occurred throughout the dentate gyrus in response to stimuli (Stim) applied to the site indicated. Recording sites are indicated by open circles at the base of the arrows. A MFV evoked using the same stimulus is shown at lower left. It was recorded in the s. lucidum of Ca3b, 0.97 mm from the stimulation site. *B*, 'anti-/orthodromic' conduction, in which impulses are conducted antidromically along collaterals of mossy fibres and then orthodromically to hippocampal pyramidal cells via mossy fibre axon trunks. *C*, latencies of GCPSs as a function of distance between stimulus and recording electrodes. The GCPSs were elicited by stimuli applied to the s. granulosum and recorded in the suprapyramidal blade or at the crest. Superimposed is the regression line (dashed) derived from the analogous data in Fig. 4C.

orthodromically. This apparent discrepancy could be a result of differences in the subsets of mossy fibre axons activated by stimuli applied to the dentate gyrus and to the s. lucidum. Many (perhaps all) mossy fibres have collaterals in the hilus (Ramón y Cajal, 1911; Claiborne *et al.* 1986), collaterals that terminate in a dense projection closely apposed to the s. granulosum (Fig. 6 of Johnston & Brown, 1983). If these collaterals were activated by electrical shocks intended to stimulate granule cells, they would then conduct impulses antidromically to their own parent mossy fibre trunks. Thus, granule cells remote from a stimulation site would be activated

via their collaterals, and impulses would be conducted to the hippocampus, first by travelling antidromically along the hilar collaterals of mossy fibres, and then via orthodromic conduction along the main axon trunks (Fig. 6C). We refer to this as the 'anti-/orthodromic' conduction route. Based on the lengths of reconstructed mossy fibre collaterals (Claiborne *et al.* 1986), impulses following the anti-/orthodromic route would travel up to 1 mm farther than impulses conveyed to the same place in hippocampus by the direct orthodromic route. This extra distance could account for 1.5 ms of surplus latency, and possibly more, if the conduction velocity in collaterals were to be significantly less than in mossy fibre axon trunks.

Consistent with this hypothesis, stimuli applied to one point in the s. granulosum were found to evoke remote GCPs elsewhere in the s. granulosum (Fig. 6A). Such 'remote GCPs' were recorded from eleven pairs of stimulus and recording sites in five slices. They were not volume-conducted potentials; as seen at the lower right of Fig. 6A, the amplitude of the potential in the infrapyramidal blade exceeds that recorded in the hilus, even though the former potential was recorded farther from the stimulus site. Furthermore, laminar profiles of remote GCPs were identical to profiles of GCPs elicited by stimulation of the s. lucidum (*cf.* Figs 4B and 6A). Remote GCPs were elicited by stimuli as low as 0.2 mA, and their amplitudes were close to maximal at stimulus currents of 1 mA or greater (data not shown); thus remote granule cells were activated by stimuli no different from those used to evoke MFVs and low-amplitude EPSCs. These data show that the conduction along the antidromic leg of the proposed anti-/orthodromic conduction route occurs under conditions typical of those used in studies of mossy fibre EPSCs. Latencies of remote GCPs exhibited a dependence on conduction distance similar to that observed for other GCPs (Fig. 6C). Thus there appears to be no gross difference in conduction velocity between mossy fibre axon trunks and collaterals.

Effects of manipulations intended to minimize the extent of anti-/orthodromic conduction

From the above hypothesis, one would expect that stimuli applied near the hippocampal termination of the suprapyramidal blade of the s. granulosum would produce MFVs with longer durations than those elicited by stimuli applied at the crest because impulses initiated at the crest would travel nearly the same distance regardless of whether they followed a direct orthodromic or an anti-/orthodromic route. We found, however, that MFVs elicited by crest stimulation lasted nearly as long as other MFVs (Fig. 5A and Db). The mean duration for these was 3.0 ms ($n = 4$), only 0.2 ms shorter than other MFVs and 1.7 ms longer than the mean SCFV duration. Moreover, EPSCs could have complex, inflected rising phases even when evoked by stimulation of the crest (Fig. 1C).

From the anti-/orthodromic hypothesis, one would also predict that long MFVs elicited by stimuli applied near the hippocampal termination of the suprapyramidal blade would be shortened by lesions such as 'cut 1' in Fig. 7A, since such lesions would transect hilar mossy fibre axon collaterals. To test this prediction, lesions of this sort were made in nine slices and effects on MFV shape and duration were examined. In these experiments, hilar cuts passed within 130–370 μm of the stimulus electrode (mean = 240 μm). 'Cut 1' was made with a stream of ACSF ejected from

a micropipette in five experiments (e.g. Fig. 7*C* and *D*). When this method was used, the stimulus and recording electrodes were left in place while making the lesion so that direct comparison could be made between MFVs before and after. Use of a fluid stream appeared to result in a complete or nearly complete transection of axons;

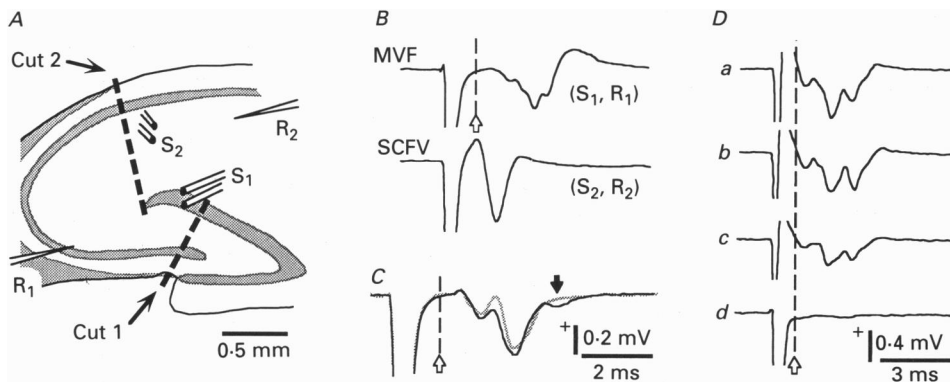


Fig. 7. Cutting hilar collaterals does not eliminate late MFV components. *A*, general anatomical arrangement for the cut-hilus experiments, and the specific anatomy for the records in part *B*. *B*, a MFV and a SCFV elicited and recorded with electrodes at sites indicated in part *A* (S_1 and R_1 for the MFV, S_2 and R_2 for the SCFV). Both cuts were made with a razor blade. For parts *C* and *D*, cut 2 was not made and cut 1 was made with a fluid stream (see text). *C*, the most extreme MFV shortening observed. MFVs were recorded before (black waveform) and after (grey waveform) cutting the hilus. Cutting eliminated a small, late component (filled, downward arrow). *D*, data from a different slice in which cutting did not shorten the MFV. *Da* was recorded prior to making any cuts, and *Db* and *Dc* after making cuts that passed within 345 and 125 μm of the stimulation site, respectively. *Dd* is a control recorded after applying the fluid stream to the slice between the stimulus and recording sites. The stimulus protocol was the same throughout; the difference in the stimulus artifact in *Dd* may have been a consequence of decreasing resistance between stimulating and recording electrodes by removing some of the intervening slice material. For part *B*, neurotransmission was blocked with D-APV and CNQX; for parts *C* and *D* it was blocked with Ca^{2+} -free, high- Mg^{2+} ACSF. The scale indications at lower right apply to both parts *B* and *D*.

very little material remained visible along the path of the applied stream, and MFVs were abolished if the fluid stream was applied between the stimulus and recording sites (Fig. 7*Dd*). However, to corroborate the results obtained with this method, a different and more rigorous method of cutting was used in four additional experiments (e.g. Fig. 7*B*): cuts were made with a razor blade, either before placing the slice in the recording chamber or with it temporarily removed. Pre- and post-lesion MFVs were recorded in one of these latter four experiments. As a precaution, perforant path axons were also lesioned in some experiments (Fig. 7*A*, 'cut 2'); this latter manipulation was without apparent effect on MFV durations.

Considering the nine cut-hilus experiments as a group, the mean MFV duration was 2.6 ± 0.4 ms, 0.6 ms less than the mean MFV duration in unlesioned slices. This difference was significant at the level of $P < 0.025$, based on a one-tailed, independent-samples *t* test (Spatz & Johnston, 1984). Similarly, there was a small, but statistically significant reduction in the MFV duration in the six cases in which

pre- and post-lesion data were recorded. For this group, the mean MFV duration was 3.0 ± 0.4 ms before making cuts and 2.7 ± 0.4 ms afterwards. This reduction was significant at the level of $P < 0.05$, based on a one-tailed, dependent-samples t test.

Although these findings indicate that anti-/orthodromic conduction is the cause of a portion of the observed MFV duration and complexity, they also left most of that duration and complexity unexplained. After making the razor cuts in Fig. 7A, one would expect there to be, at most, 100–200 μm of additional conduction distance resulting from anti-/orthodromic conduction, and yet the MFV recording from this slice has multiple components with up to 3 ms of surplus latency (Fig. 7B). In Fig. 7C, we present the most extreme case of MFV shortening brought about by cutting the hilus. Although the duration of this MFV was reduced by 0.7 ms, the overall effect of the lesion on the waveform was decidedly minor. In Fig. 7D, an alternative example is presented in which cutting did not reduce MFV duration and complexity appreciably, even when the cut was made so close to the stimulation site that the MFV elicited was diminished in amplitude. As a group, the MFVs in cut slices were much longer and more complex than SCFVs (Fig. 5D). These data indicate that a second mechanism, other than anti-/orthodromic conduction, was the major cause of asynchrony and surplus latency of mossy fibre activity.

The possibility was considered that MFVs were prolonged as a result of some aspect of granule cell physiology. To test this, in addition to lesioning of hilar collaterals, the granule cells near the stimulation site were either cut away or crushed in four slices. The stimulus electrodes were then pressed against the hilar side of the cut or crush. This manipulation had no appreciable effect on the complexity or duration of MFVs (data not shown). The mean MFV duration after granule cell crush was 2.5 ms ($n = 4$), virtually the same as the mean for lesioned slices with granule cells intact.

DISCUSSION

These data indicate that asynchrony of mossy fibre input is a major factor determining the shape and duration of the rising phase of mossy fibre EPSCs evoked by bulk stimuli applied to granule cells and/or mossy fibres in the dentate gyrus. Bulk stimulation elicited MFVs and mossy fibre EPSCs with multiple components exhibiting variable amounts of 'surplus' latency, latency in addition to that expected for conduction of impulses directly to hippocampus along mossy fibre axon trunks. Part of this surplus latency is a consequence of 'anti-/orthodromic' conduction: mossy fibre impulses travel to the hippocampus by direct and indirect routes, with the latter involving hilar collaterals of mossy fibres. However, the data strongly suggest that additional asynchrony and surplus latency arises by a second mechanism, one that is inherent in the way mossy fibre axons or boutons function.

Authenticity of MFVs

Much of our interpretation rests upon analysis of the shape of MFV waveforms, and this in turn depends critically upon authenticity of these waveforms. Late, contaminating potentials of non-mossy fibre origin superimposed upon true MFVs could be erroneously interpreted as evidence for late, asynchronous mossy fibre activity. Spiking pyramidal cell somata situated near a MFV recording site could

generate laminar profiles similar to those of MFVs, and thus be especially problematic. However, synaptic input would not have caused pyramidal cells to spike under the conditions of these experiments because neurotransmission was blocked by omitting Ca^{2+} from the ACSF or by the addition of glutamate receptor antagonists. We considered the alternative possibility of direct activation of CA3c pyramidal cells, either via their apical dendrites or via their local collateral axons, some of which project to the hilus (Ishizuka, Weber & Amaral, 1990). If this had occurred, one would expect it to be more pronounced when high-intensity stimuli were applied to the suprapyramidal blade of the s. granulosum. However, late MFV components were present at threshold stimulus intensities (Fig. 5C), and MFVs were long and complex even when stimuli were applied to the crest of the dentate gyrus, a location where direct stimulation of hippocampal pyramidal cells would have been most unlikely. It is therefore concluded that pyramidal cell population spikes did not contaminate MFVs to a significant extent.

EPSC components as unitary EPSCs

A primary goal of this investigation was to account for long mossy fibre EPSC rise times. In the light of the MFV data, however, it would appear that when bulk stimulation is used, *long* EPSC rise times should be the expected and *brief* EPSC rise times require an explanation. MFV negative phases were always longer than 2.2 ms, whereas 35% of the EPSCs in our sample had rise times between 0.6 and 2 ms. We attribute this apparent discrepancy to differences in the numbers of active fibres sampled by these recording methods. MFVs were probably generated by the summed activity of relatively large numbers of active mossy fibres, whereas our low-amplitude EPSCs were driven by input from only a few active mossy fibres. This interpretation is consistent with anatomical considerations (Amaral, Ishizuka & Claiborne, 1990), the small amplitudes of the EPSCs in our sample, and the complexity and trial-by-trial variability of response waveforms. We propose that complex EPSCs with long overall rise times occurred in those cells that happened to receive inputs dispersed throughout the 2–4 ms during which mossy fibres were active, and that brief and apparently simple EPSCs occurred in those cells that happened to receive inputs of nearly the same latency.

For compound EPSCs driven by small numbers of inputs, a plausible consequence of input asynchrony would be that some unitary EPSCs (EPSCs driven by input from a single presynaptic bouton) would be manifest as distinct components within compound EPSCs. Consistent with this hypothesis, there was a similarity in time course and amplitude between our most rapidly rising EPSCs, our rapid components within complex EPSCs, and the EPSCs recorded and proposed to be unitary by Jonas & Sakmann (1991). There was further consistency between the previous and present results with respect to the EPSC latencies. EPSCs recorded by Jonas & Sakmann had mean latencies from 1.9 to 6.4 ms. This wide range implies a pattern of 'surplus latency' similar to that observed for components of EPSCs and MFVs in the present study. We derive the following tentative conclusions from the available data (past and present): unitary mossy fibre EPSCs (1) acquire significant latency in addition to that directly attributable to orthodromic conduction delay, (2) rise in 0.3–1.5 ms, (3) exhibit large trial-by-trial variations in amplitude, and (4) can have amplitudes as large as 350 pA.

There are at least three mechanisms that could account for large trial-by-trial variations in the amplitudes of unitary EPSC components. (1) They may have been the result of random fluctuation in the quantal content of unitary EPSCs. However, variation of a component's amplitude between 0 and 350 pA (Fig. 1*B*) would imply either remarkably large quanta, or some mechanism that causes the probability of release at separate release sites within a bouton to co-vary. (2) Components that failed sporadically may have been driven by input from mossy fibres (or their parent granule cells) that were not consistently brought to threshold by the stimulus. This could be the case for cells and axons situated on the edge of the region within which stimuli were consistently effective. (3) Amplitude variations may have resulted from fluctuation in the extent to which axon spikes succeeded in depolarizing mossy fibre boutons (see below).

Site(s) of desynchronization

Desynchronization of mossy fibre impulses could occur, hypothetically, at any of three sites: (1) where impulses were initiated, (2) along mossy fibre axons, while impulses were en route to the boutons, or (3) at the terminal boutons. With regard to the first of these sites, it was considered that asynchrony may have been a consequence of direct stimulation of granule cell somata (as opposed to direct stimulation of axons, as when SCFVs are elicited). This hypothesis was dismissed, however, because crush or resection of granule cells did not result in shorter MFVs. As for desynchronization of impulses en route, these could be caused by differences in conduction velocity within mossy fibre populations. However, this hypothesis predicts broadening of antidromically activated GCPSs with increasing conduction distance, and very little of such broadening occurred (Fig. 4*C*).

The experimental result provided stronger, though qualified, support for the hypothesis that impulses were desynchronized en route by 'anti-/orthodromic' conduction. Stimuli identical to those used in studies of mossy fibre EPSCs are clearly sufficient to initiate impulse conduction along the antidromic leg of the anti-/orthodromic route, as indicated by the spatial distributions of GCPSs elicited by stimuli applied to the s. granulosum (Fig. 6). In addition, cutting the hilus reduced MFV durations. However, the effect of these cuts was relatively small. The results make it clear that some mossy fibre impulses have surplus latency as a consequence of anti-/orthodromic conduction. However, the data also demonstrate that anti-/orthodromic conduction makes only a small contribution to the overall extent of desynchronization and surplus latency.

Na⁺ spikes in mossy fibre 'giant' boutons?

Persistence of late MFV components after cuts was one of two findings left unexplained by the anti-/orthodromic hypothesis. The other was that application of stimuli to the crest of the dentate gyrus did not elicit short and simple MFVs, nor did it assure that EPSCs would have brief and simple rising phases. To account for these findings, we propose that there is an appreciable delay as impulses invade mossy fibre boutons. There is likely to be a very large impedance mismatch at the junction between mossy fibre axons and their boutons because these structures differ in diameter by roughly 15- to 20-fold (Hamlyn, 1962). This impedance mismatch would be accentuated by the fact that mossy fibre boutons are convoluted, wrapping

around the thorny excrescences of the dendrites with which they synapse (Chicurel & Harris, 1992). These convolutions would add to bouton capacitance, which would further impede the spread of the axon spike into the bouton. The present physiological data and the pre-existing anatomical data are consistent with the following hypotheses: (1) passive depolarization of mossy fibre boutons is inadequate to bring about neurotransmitter release; (2) mossy fibre boutons actively spike to overcome the impedance mismatch; (3) bouton spikes typically occur after appreciable invasion delays (4) individual invasion delays differ among mossy fibres; (5) late MFV components are generated by bouton spikes (voltage-gated Na^+ current entering mossy fibre boutons), rather than by axon spikes (current entering mossy fibre axons).

From the present data, we infer that bouton spike invasion delays vary between roughly 1 and 3 ms. Variability in this delay would be consistent with anatomical data showing that the connection between mossy fibre axons and boutons varies greatly within mossy fibre populations (Blackstad & Kjaerheim, 1961). We propose that mossy fibre bouton spikes are mediated primarily by Na^+ , rather than Ca^{2+} current because MFVs recorded in the presence and the absence of extracellular Ca^{2+} were similar. Consistent with this interpretation, Na^+ spikes have been recorded extracellularly from individual mossy fibre boutons using loosely attached patch electrodes (R. Gray & D. Johnston, personal communication). The bouton spike hypothesis is also consistent with another experimental finding, that MFV waveform shapes changed with small changes in the recording position. This sensitivity to position suggests that MFVs were generated by relatively small numbers of elements, be they boutons or axons. Mossy fibre boutons would be better suited to fill this role. Because of their size, individual boutons would probably make relatively large contributions to the total extracellular potential (the MFV), and any particular recording site would be in close proximity to far fewer boutons than axons.

The bouton spike hypothesis proposes, in effect, an extra step in the sequence of events by which granule cell activation results in excitatory input to CA3 pyramidal cells. By analogy with antidromic invasion of cell somata (Lipski, 1981), invasion into mossy fibre boutons should succeed or fail depending upon the balance between the activity of voltage-gated cation channels and shunting conductances. Thus, changes in synaptic efficacy (such as occur, for example, during mossy fibre long-term potentiation) could be the result of alterations in the probability of bouton spike invasion brought about by modification of the excitability or conductance of Na^+ channels in mossy fibre boutons.

Methodological implications of these findings

Based on the data in this and other recent studies, it is highly questionable whether the 3 ms rise time criterion can provide a valid basis for discrimination between pure mossy fibre EPSCs and EPSCs contaminated by input from pyramidal cell collateral projections. EPSCs that are driven by collaterals ('collateral EPSCs') often appear as single-component responses that rise in less than 3 ms (Langdon *et al.* 1991; Williams & Johnston, 1991). Therefore, if rise times are to serve as a useful criterion for identifying authentic mossy fibre EPSCs, the 3 ms rejection threshold must be revised to a new value determined by the lower boundary of the range of collateral EPSC rise times. This boundary is likely to be near 1 ms. In the studies by

Langdon *et al.* (1991) and Williams & Johnston (1991), the fastest collateral EPSCs rose in about 2 ms. However, inputs to distal dendrites were selectively activated in these studies, as a consequence of measures taken to avoid activation of mossy fibres. In a different study, in which proximal collateral inputs to CA1 pyramidal cells were selectively activated, the lower limit of rise times was close to 1 ms (Hestrin *et al.* 1990), and similar results have been obtained in a study of fibrial input to CA3 pyramidal cells (D. A. Henze, W. E. Cameron & G. Barrionuevo, unpublished).

If all EPSCs with rise times greater than 1 ms are rejected, experimental yields are likely to be very low; only a small fraction of the EPSCs in the present study satisfied this criterion. It would therefore be useful to have an alternative or adjunct criterion. We have considered, as one such adjunct, the use of response latencies. However, our data show that exact latencies of pure mossy fibre EPSCs cannot be predicted from conduction distances. Since mossy fibre EPSCs often appear as the sum of rapid components with individual rise times less than 1 ms, an alternative approach would be to tentatively accept such compound responses as authentic, provided that they retain the same shape during exposure to suppressing media, such as ACSF low in Ca^{2+} and high in Mg^{2+} or ACSF containing glutamate receptor blockers.

We are pleased to acknowledge Dr William E. Cameron for his useful comments regarding interpretation of these data. This work was supported by grants from the Human Frontiers Research Program, NIMH MH00944, NINDS NS24288 and NS01196, AFOSR 91-0441 and NIMH MF45156.

REFERENCES

- AMARAL, D. G., ISHIZUKA, N. & CLAIBORNE, B. (1990). Neurons, numbers and the hippocampal network. *Progress in Brain Research* **83**, 1–11.
- AMARAL, D. G. & WITTER, M. P. (1989). The three-dimensional organization of the hippocampal formation: a review of anatomical data. *Neuroscience* **31**, 471–591.
- ASCHER, P. & NOWAK, L. (1988). Quisqualate- and kainate-activated channels in mouse central neurones in culture. *Journal of Physiology* **399**, 227–245.
- BARRIONUEVO, G., KELSO, S. R., JOHNSTON, D. & BROWN, T. H. (1986). Conductance mechanism responsible for long-term potentiation in monosynaptic and isolated excitatory synaptic inputs to hippocampus. *Journal of Neurophysiology* **55**, 540–550.
- BLACKSTAD, T. W. & KJÆRHEIM, A. (1961). Special axo-dendritic synapses in the hippocampal cortex: Electron and light microscopic studies in the layer of mossy fibers. *Journal of Comparative Neurology* **117**, 133–159.
- BORMANN, J., HAMILL, O. P. & SAKMANN, B. (1987). Mechanism of anion permeation through channels gated by glycine and γ -aminobutyric acid in mouse cultured spinal neurones. *Journal of Physiology* **385**, 243–286.
- BROWN, T. H. & JOHNSTON, D. (1983). Voltage-clamp analysis of mossy fiber synaptic input to hippocampal neurons. *Journal of Neurophysiology* **50**, 487–507.
- BROWN, T. H. & ZADOR, A. M. (1990). Hippocampus. In *The Synaptic Organization of the Brain*, 3rd edn, ed. SHEPHERD, G. M., pp. 346–388. Oxford University Press, New York, NY, USA.
- CHEN, Q. X., STELZER, A., KAY, A. R. & WONG, R. K. S. (1990). GABA_A receptor function is regulated by phosphorylation in acutely dissociated guinea-pig hippocampal neurones. *Journal of Physiology* **420**, 207–221.
- CHICUREL, M. E. & HARRIS, K. M. (1992). Three-dimensional analysis of the structure and composition of CA3 branched dendritic spines and their synaptic relationships with mossy fiber boutons in the rat hippocampus. *Journal of Comparative Neurology* **325**, 169–182.
- CLAIBORNE, B. J., AMARAL, D. G. & COWAN, W. M. (1986). A light and electron microscopic analysis of the mossy fibers of the rat dentate gyrus. *Journal of Comparative Neurology* **246**, 435–458.

- EDWARDS, F. A., KONNERTH, A., SAKMANN, B. & TAKAHASHI, T. (1989). A thin slice preparation for patch clamp recordings from neurones of the mammalian central nervous system. *European Journal of Physiology* **414**, 600–612.
- FINKEL, A. S. & REDMAN, S. J. (1983). The synaptic current evoked in cat spinal motoneurons by impulses in single group Ia axons. *Journal of Physiology* **342**, 615–632.
- GRIFFITH, W. H., BROWN, T. H. & JOHNSTON, D. (1986). Voltage-clamp analysis of synaptic inhibition during long-term potentiation in hippocampus. *Journal of Neurophysiology* **55**, 767–775.
- HAMLIN, L. H. (1962). The fine structure of mossy fiber endings in the hippocampus of the rabbit. *Journal of Anatomy* **96**, 112–120.
- HESTRIN, S., NICOLL, R. A., PERKEL, D. J. & SAH, P. (1990). Analysis of excitatory synaptic action in pyramidal cells using whole-cell recording from rat hippocampal slices. *Journal of Physiology* **422**, 203–225.
- HILLE, B. (1992). *Ionic Channels of Excitable Membranes*, pp. 337–361. Sinauer Associates, Inc., Sunderland, MA, USA.
- HUMPHREY, D. R. (1968). Re-analysis of the antidromic cortical response. II. On the contribution of cell discharge and PSPs to the evoked potentials. *Electroencephalography and Clinical Neurophysiology* **24**, 115–129.
- ISHIZUKA, N., WEBER, J. & AMARAL, D. G. (1990). Organization of intrahippocampal projections originating from CA3 pyramidal cells in the rat. *Journal of Comparative Neurology* **295**, 580–623.
- JOHNSTON, D. & BROWN, T. H. (1983). Interpretation of voltage-clamp measurements in hippocampal neurons. *Journal of Neurophysiology* **50**, 464–486.
- JOHNSTON, D., WILLIAMS, S., JAFFE, D. & GRAY, R. (1992). NMDA-receptor-independent long-term potentiation. *Annual Review of Physiology* **54**, 489–505.
- JONAS, P. & SAKMANN, B. (1991). Unitary stimulus-evoked postsynaptic currents in CA3 pyramidal cells of rat hippocampal slices as resolved by patch clamp techniques. *Journal of Physiology* **446**, 515P.
- KLEE, M. & RALL, W. (1977). Computed potentials of cortically arranged populations of neurons. *Journal of Neurophysiology* **40**, 647–666.
- LANGDON, R. B., JOHNSON, J. W. & BARRIONUEVO, G. (1991). Time-course and plasticity of rat hippocampal CA3 pyramidal cell responses to input from recurrent collaterals examined by whole-cell recordings. *Society for Neuroscience Abstracts* **17**, 1330.
- LANGDON, R. B., JOHNSON, J. W. & BARRIONUEVO, G. (1992). Input asynchrony prolongs the rising phase of mossy fiber-evoked EPSCs in rat hippocampal CA3 pyramidal cells. *Society for Neuroscience Abstracts* **18**, 1350.
- LANGDON, R. B. & SUR, M. (1990). Components of field potentials evoked by white matter stimulation in isolated slices of primary visual cortex: Spatial distributions and synaptic order. *Journal of Neurophysiology* **64**, 1484–1501.
- LANGDON, R. B. & SUR, M. (1992). The effects of selective glutamate receptor antagonists on synchronized firing bursts in layer III of rat visual cortex. *Brain Research* **599**, 283–296.
- LIPSKI, J. (1981). Antidromic activation of neurones as an analytic tool in the study of the central nervous system. *Journal of Neuroscience Methods* **4**, 1–32.
- LLINÁS, R., BLOEDEL, J. R. & HILLMAN, D. E. (1969). Antidromic invasion of Purkinje cells in frog cerebellum. *Journal of Neurophysiology* **32**, 881–891.
- LORENTE DE NÓ, R. (1934). Studies of the structure of the cerebral cortex. II. Continuation of the study of the ammonic system. *Journal für Psychologie und Neurologie* **46**, 113–177.
- LORENTE DE NÓ, R. (1947). Action potential of the motoneurons of the hypoglossus nucleus. *Journal of Cellular and Comparative Physiology* **29**, 207–287.
- NELSON, P. G., PUN, R. Y. K. & WESTBROOK, G. L. (1986). Synaptic excitation in cultures of mouse spinal cord neurones: receptor pharmacology and behaviour of synaptic currents. *Journal of Physiology* **372**, 169–190.
- RAMÓN Y CAJAL, S. (1911). *Histologie du système nerveux de l'homme et des vertèbres*. Tome II. Maloine, Paris.
- SPATZ, C. & JOHNSTON, J. O. (1984). *Basic Statistics*, 3rd edn. Brooks/Cole, Monterey, CA, USA.
- WILLIAMS, S. H. & JOHNSTON, D. (1991). Kinetic properties of two anatomically distinct excitatory synapses in hippocampal CA3 pyramidal neurons. *Journal of Neurophysiology* **66**, 1010–1020.